Risk Analysis, Vol. 42, No. 2, 2022 DOI: 10.1111/risa.13762

System Analysis of Wildfire-Water Supply Risk in Colorado, USA with Monte Carlo Wildfire and Rainfall Simulation

Benjamin M. Gannon,[1,*] Yu Wei,[1] Matthew P. Thompson,[2] Joe H. Scott,[3] and Karen C. Short[4]

Water supply impairment from increased contaminant mobilization and transport after wildfire is a major concern for communities that rely on surface water from fire-prone watersheds. In this article we present a Monte Carlo simulation method to quantify the likelihood of wildfire impairing water supplies by combining stochastic representations of annual wildfire and rainfall activity. Water quality impairment was evaluated in terms of turbidity limits for treatment by modeling wildfire burn severity, postfire erosion, sediment transport, and suspended sediment dilution in receiving waterbodies. Water supply disruption was analyzed at the system level based on the impairment status of water supply components and their contributions to system performance. We used this approach to assess wildfire-water supply impairment and disruption risks for a system of water supply reservoirs and diversions in the Front Range Mountains of Colorado, USA. Our results indicate that wildfire may impair water quality in a concerning 15.7–19.4% of years for diversions from large watersheds. Reservoir impairment should be rare for off-network reservoirs—ranging from at most 0.01% of years for large reservoirs to nearly 2% of years for small reservoirs. System redundancy meaningfully reduced disruption risk for alternative conveyance routes (4.3–25.0% reduction) and almost eliminated disruption risk for a pair of substitutable terminal sources (99.9% reduction). In contrast, dependency among reservoirs on a conveyance route nearly doubled risk of disruption. Our results highlight the importance of considering water system characteristics when evaluating wildfire-water supply risks.

KEY WORDS: System analysis; water supply impairment; wildfire risk

1. INTRODUCTION

Wildfire is a growing concern in source water management due to recent high-profile incidents of infrastructure and water quality impairment and predictions that similar events will become more frequent and severe in regions with projected increases in wildfire activity (Hallema et al., 2019; Martin, 2016; Sankey et al., 2017; Smith, Sheridan, Lane, Nyman, & Haydon, 2011). This concern has motivated diverse efforts to characterize wildfire-water supply risks. Global and regional assessments have built awareness of where wildfire poses the greatest threat to water supplies by combining measures of fire activity, watershed response, and water utilization to map relative indices of risk (Robinne et al., 2018, 2019; Thompson , Scott, Langowski et al., 2013). Local assessments have gravitated toward coupled

[1]Department of Forest and Rangeland Stewardship, Colorado State University, Fort Collins, CO, USA.
[2]Rocky Mountain Research Station, USDA Forest Service, Fort Collins, CO, USA.
[3]Pyrologix, Missoula, MT, USA.
[4]Rocky Mountain Research Station, USDA Forest Service, Missoula, MT, USA.
[*]Address correspondence to Benjamin Gannon, Department of Forest and Rangeland Stewardship, Colorado State University, 1472 Campus Delivery, Fort Collins, CO 80523, USA; benjamin.gannon@colostate.edu

wildfire-watershed models to help communities quantify risk and mitigation effectiveness in terms of reservoir sedimentation and associated costs (Buckley et al., 2014; Elliot, Miller, & Enstice, 2016; Gannon et al., 2019; Jones et al., 2017). In contrast, risk of water quality impairment (hereafter "impairment risk") remains poorly quantified despite recognition that source impairment is usually the most significant short-term water management challenge after wildfire (Sham, Tuccillo, & Rooke, 2013). Most worrisome is the potential for wildfire to disrupt municipal water supply (hereafter "disruption risk") by severely impairing one or more critical sources. Analyzing disruption risk would benefit from improvements to physical modeling of contaminant mobilization, transport, and dilution to assess water supply impairment (Nunes et al., 2018; Rhoades, Nunes, Silins, & Doerr, 2019) and a systems perspective to evaluate impairment consequences for communities with multiple sources (Haimes, 2012).

Wildfire-related increases in sediment, carbon, nutrients, metals, and other contaminants can render water expensive or unfit to treat at high concentrations (Abraham, Dowling, & Florentine, 2017; Nunes et al., 2018; Rust, Saxe, McCray, Rhoades, & Hogue, 2019; Smith et al., 2011). Water erosion is the dominant process mobilizing postfire contaminants, especially in montane watersheds (Abraham et al., 2017; Nunes et al., 2018; Smith et al., 2011). In our study region, surface water collection and treatment systems are poorly adapted to high concentrations of suspended sediment, which can interfere with conveyance, filtration, and treatment (Sham et al., 2013; Smith et al., 2011). Suspended sediment is also a reasonable proxy for other contaminants because carbon and nitrogen tend to mobilize in response to the same intense rainfall that triggers erosion (Murphy, Writer, McCleskey, & Martin, 2015) and because some contaminants, such as phosphorus, are adsorbed to the transported sediments (Smith et al., 2011). Evaluating impairment in terms of contaminant concentration limits for treatment provides a clear means to account for varying water supply susceptibility owing to the effect of water body size on concentration (Nunes et al., 2018; Smith et al., 2011). Recently, Robinne et al. (2019) addressed impairment susceptibility using a distance-based decay function that approximates the trend of increasing dilution with watershed size. Alternatively, quantitative predictions of postfire contaminant loads can be used to evaluate water quality impairment by calculating contaminant concentrations in the receiving waterbody and comparing them to common water quality standards (Murphy et al., 2015; Smith et al., 2011) as has been demonstrated for debris flow-generated sediments in Australia (Langhans et al., 2016).

The threshold dependent nature of water quality impairment implies that it is important for risk assessment to account for the spatial and temporal intersections of wildfire and rainfall activity with sufficient magnitudes to mobilize problematic quantities of contaminants into source water bodies. Jones, Nyman, and Sheridan (2014) estimated the frequency of wildfire intersections with rainstorms above a typical threshold for debris flow occurrence in Australia using a germ-grain model, but did not consider the spatial variability in erosion and sediment transport potential to water supplies that other studies suggest is considerable in heterogenous watersheds (e.g., Elliot et al., 2016; Gannon et al., 2019). Monte Carlo simulation of discrete wildfire events provides an alternative means to describe the spatial and temporal variability in watershed area burned and effects (Haas, Thompson, Tillery, & Scott, 2017; Thompson, Gilbertson-Day, & Scott, 2016; Thompson, Scott, Kaiden, & Gilbertson-Day, 2013) including water quality outcomes (Langhans et al., 2016). In our study region, the intense summer thunderstorms that are responsible for most erosion (Benavides-Solorio & MacDonald, 2005; Moody & Martin, 2009) are also highly variable in space and time (Kampf, Brogan, Schmeer, MacDonald, & Nelson, 2016; Murphy et al., 2015). Previous risk assessments have addressed rainfall variability by reporting watershed response predictions for several rainfall return intervals (Gannon et al., 2019; Haas et al., 2017; Jones et al., 2017), but accounting for spatial and temporal wildfire and rainfall activity in a combined Monte Carlo analysis would more accurately convey how variability in the major stochastic drivers combine to influence erosion and contaminant concentrations. Event-based Monte Carlo methods are particularly attractive for their ability to simulate frequency distributions of disturbance magnitudes that can be used for traditional engineering risk and reliability analyses (Singh, Jain, & Tyagi, 2007).

Wildfire-water supply risk assessment has so far lacked a systems perspective for evaluating the consequences of water quality impairment despite the demonstrated utility of alternative sources for moderating wildfire impacts (Writer et al., 2014) and recommendations for this as an approach to engineer water system reliability (Martin, 2016; Murphy et al.,

2015; Sham et al., 2013). Event-based Monte Carlo simulation of wildfire and rainfall is well suited for systems risk analysis because wildfire activity and resulting postfire water quality can be tracked across component water supplies to determine their impairment states, and the resulting consequence for system performance can be evaluated in light of the component states and functions (Haimes, 2012). The critical contribution of event-based simulation is to define the joint probabilities of impairment across system components, which would take centuries to accurately define from observational data. The systems framework can represent both redundancies, such as alternative water sources, and dependencies, such as conveyance paths with multiple impact points. Accounting for these functional relationships should improve risk assessment for complex water systems and provide a means to evaluate the effects of operational or infrastructure changes on system reliability.

Here we demonstrate an event-based Monte Carlo risk analysis to estimate the probability of water impairment and system supply disruption for a multisource water system in Colorado. To account for key uncertainties, we combined 10,000 years of stochastically simulated wildfire and rainfall activity to model poststorm turbidity for water supply streams and reservoirs with coupled burn severity, erosion, and sediment transport models. We then assessed impairment risk for individual water supplies as the annual probability of exceeding suspended sediment standards for water treatment. System supply disruption was assessed by evaluating whether water demands can be met based on water supply impairment states and contributions to system performance. We applied this framework to assess disruption risk for subsystems with redundancy and dependency to illustrate how wildfire risk may either be mitigated or magnified by the functional relationships between water system components.

2. METHODS

2.1. Water System

The study water system is in the Front Range Mountains of Colorado, United States. The names of the communities, infrastructure, and other geographic features within the analysis area are withheld for security reasons. The water system consists of the primary diversion for a community and the conveyance system and terminal reservoirs for a regional water project that supplements the community's primary source (Fig. 1; Table I). The total upland contributing area to the system is 2,127 km^2. Elevation ranges from 1,616 to 4,343 m above sea level. The watersheds are steep; 68.5% of the area is greater than 20% slope and 29.2% is greater than 40% slope. The climate is continental with warm dry summers and cold winters. Total annual precipitation, which increases with elevation, ranges from 351 to 1325 mm (PRISM, 2014). Snow amount and seasonality varies widely across the study area; average snow persistence between January 1st and July 3rd ranges from 10.7% in the low foothills to 93.6% in the high mountains (Moore, Kampf, Stone, & Richer, 2015). Thunderstorms between June and October provide the majority of erosive power (Benavides-Solorio & MacDonald, 2005). Forest is the dominant land cover (73.1%) followed by barren alpine (9.6%), grassland (7.8%), and shrubland (7.0%) (LANDFIRE, 2016). The Colorado Front Range has a history of wind-driven fires that have burned large areas at moderate and high severity resulting in problematic erosion, reservoir sedimentation, and degraded water quality (Graham, 2003; Moody & Martin, 2001; Murphy et al., 2015; Oropeza & Heath, 2013; Wagenbrenner, MacDonald, & Rough, 2006).

2.2. Monte Carlo Simulation

Probability of exceeding water quality thresholds for treatment and conveyance was assessed with Monte Carlo simulation of poststorm suspended sediment concentration (SSC) over 10,000 years of stochastic wildfire and rainfall (Fig. 2). Wildfire activity was modeled using a combination of stochastic wildfire perimeters from the Large Fire Simulator (FSim; Finney, McHugh, Grenfell, Riley, & Short, 2011) to describe wildfire occurrence in space and time, and static predictions of crown fire activity from FlamMap 5 (Finney, Brittain, Seli, McHugh, & Gangi, 2015) to characterize the spatial variability in burn severity within fire perimeters. Interannual variability in rainfall was represented by randomly resampling historical records (Perica et al., 2013). Postfire hillslope erosion was modeled at an annual time step with a geographic information system (GIS) implementation (Theobald, Merritt, & Norman, 2010) of the Revised Universal Soil Loss Equation (RUSLE; Renard, Foster, Weesies, McCool, & Yoder, 1997) adjusted for postfire prediction in mountainous terrain (Gannon et al., 2019). Sediment transport to infrastructure was estimated with

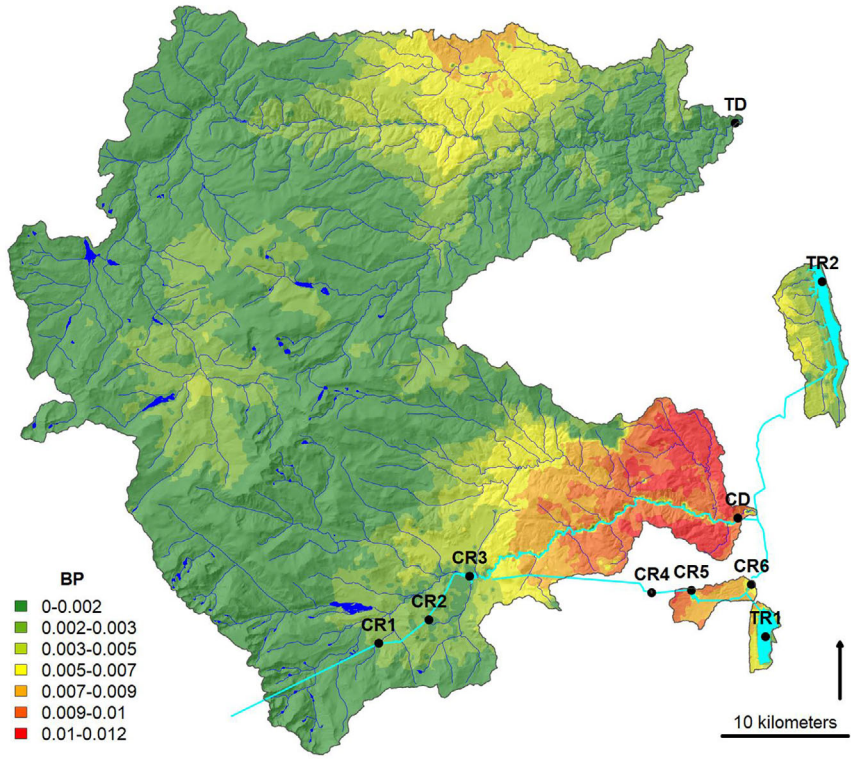

Fig 1. The study water system consists of six conveyance reservoirs (CR), two terminal reservoirs (TR), one conveyance diversion (CD), and one terminal diversion (TD). The major conveyance paths and reservoirs are cyan. Burn probability (BP) depicts the expected annual likelihood of wildfire activity across the water system.

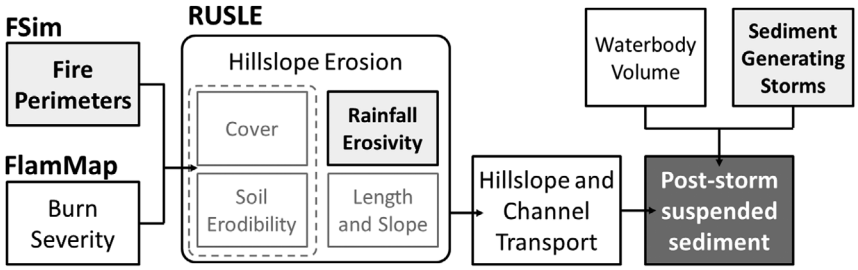

Fig 2. Stochastic components are bold with light grey fill. Annual average poststorm SSC was simulated based on spatially and temporally varying wildfire activity with FSim, static estimates of crown fire activity to approximate burn severity with FlamMap, and temporally varying rainfall from resampled historical records. Annual postfire sediment load was estimated by linking RUSLE with hillslope and channel sediment delivery ratio models. Average annual poststorm SSC was calculated by dividing the annual sediment load by the number of sediment-generating storms and evenly mixing the average storm sediment load in the receiving water body volume.

hillslope and channel sediment delivery ratio models (Frickel, Shown, & Patton, 1975; Wagenbrenner & Robichaud, 2014) adapted to the study site. Average annual poststorm SSC was calculated by dividing the annual sediment load by the number of sediment-generating storms and evenly mixing the average storm sediment load in the receiving water body volume.

2.2.1. *Fire Perimeters*

Fire occurrence was simulated with FSim (Finney et al., 2011), which models large fire occur-

Table I. Water System Infrastructure Characteristics Including Volume for Reservoirs and Discharge for Diversions. Network Placement Refers to Whether the Water Supply is Located on or off the Main Channel Network. Discharge is the Mean Annual Discharge from May through October from NHDPlus (USEPA and USGS, 2012). Burnable Contributing Area is Defined Based on Fuel Model Mapping from LANDFIRE (2016)

Code	Name	Network Placement	Volume (ha-m)	Discharge (cms)	Total Contributing Area (ha)	Burnable Contributing Area (ha)
CR1	Conveyance reservoir 1	Off	6	NA	1,148	1,126
CR2	Conveyance reservoir 2	Off	114	NA	101	81
CR3	Conveyance reservoir 3	On	378	NA	39,031	29,088
CR4	Conveyance reservoir 4	Off	12	NA	1	1
CR5	Conveyance reservoir 5	Off	269	NA	795	757
CR6	Conveyance reservoir 6	Off	94	NA	615	596
CD	Conveyance diversion	On	NA	5.5	77,810	66,100
TD	Terminal diversion	On	NA	17.1	126,739	108,606
TR1	Terminal reservoir 1	Off	13,843	NA	979	510
TR2	Terminal reservoir 2	Off	19,333	NA	4,443	3,567

rence, growth, and containment over many hypothetical fire seasons. Daily large fire occurrence is determined in FSim as a function of an artificial time series of the National Fire Danger Rating System Energy Release Component (ERC) calibrated with time series analysis of historical weather data. Fire growth is modeled using the minimum travel time algorithm (Finney, 2002) based on current fuels and topography (LANDFIRE, 2016), and daily fuel moisture, wind speed, and wind direction. Daily wind speed and direction are drawn randomly from their historical joint probability distribution by month. Fire containment is modeled based on primary fuel type and daily fire growth metrics (Finney, Grenfell, & McHugh, 2009). We used fire perimeters simulated with FSim over 10,000 hypothetical fire seasons from a separate effort to update the U.S. national probabilistic wildfire risk components (Short, Finney, Scott, Gilbertson-Day, & Grenfell, 2016). For this application, FSim was calibrated to approximate the historical fire size distribution and rate of burning by biophysical region. FSim treats fuels as stationary, so modeled wildfire activity should be interpreted as representing 10,000 possible realizations of the next fire season. The simulation year was used here only as a reference for tracking postfire erosion over multiple years of watershed recovery.

2.2.2. *Rainfall*

Two annual rainfall metrics were employed to model average storm sediment yields: rainfall erosivity was used to predict annual sediment yield from hillslope erosion (Renard et al., 1997), and the number of storms exceeding intensity thresholds for erosion (Wilson, Kampf, Wagenbrenner, & MacDonald, 2018) was used to estimate the average storm sediment yield. Both metrics were represented in the analysis by randomly sampling historical records by station to generate 10,000 years of representative rainfall activity. The historical data are from 11 rainfall gages located in the Colorado Front Range (Perica et al., 2013) that were assembled for a separate study of storm-level thresholds for erosion (Wilson et al., 2018). The individual station records are from the period 1971–2010 and the combined records account for 403 station-years of observations. We focused on rainfall during May through October because greater than 90% of hillslope erosion in the region is associated with intense summer rainfall (Benavides-Solorio & MacDonald, 2005). Rainfall erosivity, also called "rainfall-runoff erosivity," is cal-

culated as the product of storm maximum rainfall intensity and kinetic energy per unit area (Renard et al., 1997), which represent the dual triggers of hillslope erosion: sediment detachment and transport via surface runoff. For the historical data used in this analysis, annual May through October rainfall erosivity varies between 25 and 58,468 MJ mm ha^{-1} h^{-1} with a mean of 684 MJ mm ha^{-1} h^{-1}. This extreme variability is consistent with previous reports that locally powerful convective thunderstorms are responsible for the majority of erosion in the region (Kampf et al., 2016; Murphy et al., 2015; Robichaud, Lewis, Wagenbrenner, Ashmun, & Brown, 2013; Wagenbrenner et al., 2006). The 2, 10, and 100-year return interval rainfall intensities (60-min duration) calculated from the pooled station-year records are 15.6, 33.1, 91.4 mm/h, respectively. The associated number of sediment-generating storms was determined as the count of rainfall events that meet or exceed the 7 mm/h rainfall intensity threshold identified for postfire erosion in the study region by Wilson et al. (2018). The mean and maximum of the pooled observations are 4 and 18 sediment-generating storms per year during May through October.

2.2.3. Burn Severity

Crown fire activity (CFA) (Scott & Reinhardt, 2001) was modeled using FlamMap 5.0 (Finney et al., 2015) as a proxy for soil burn severity like previous studies (Gannon et al., 2019; Haas et al., 2017; Tillery, Haas, Miller, Scott, & Thompson, 2014) by mapping surface fire, passive crown fire, and active crown fire behavior to low, moderate, and high burn severity, respectively. Most area burns in the Colorado Front Range during dry and windy conditions (Graham, 2003), so CFA was modeled for 3rd percentile (low) fuel moisture (1-h 2%, 10-h 3%, 100-h 6%, herbaceous 30%, woody 63%) and 97th percentile (high) mean 1-min wind speed (39 km/h at 6 m) for the core fire season (April 1st–October 31st) from three Remote Automated Weather Stations located in the study area. Fuel moisture and wind speed percentiles were calculated with FireFamilyPlus 4.1 (Bradshaw & McCormick, 2000) and wind speed was converted from a 10-min to 1-min average based on Crosby and Chandler (1966). The wind blowing uphill option was used in FlamMap to represent a consistent worst-case scenario across aspects.

2.2.4. Watershed Modeling

The mass of postfire sediment delivered to water supplies was estimated at an annual time step by linking models of hillslope erosion, hillslope sediment transport, and channel sediment transport as described in Gannon et al. (2019) with minor modifications (Figs. 2 and 3). A summary is presented here with details reserved for the Appendix. The NHDPlus watershed network and digital elevation model were used to represent the spatial topology between sediment-producing uplands and water supplies (USEPA and USGS, 2012). Gross hillslope erosion was modeled for each burned pixel for the first three years following fire with a GIS-implementation of RUSLE (Theobald et al., 2010) by adjusting the cover and soil erodibility factors to reflect postfire conditions by burn severity and vegetation recovery over time (Gannon et al., 2019; Larsen & MacDonald, 2007). The proportion of sediment delivered from each pixel to the stream network was estimated with an empirical model of postfire hillslope sediment delivery ratio (SDR) from the western United States (annual length ratio model; Wagenbrenner & Robichaud, 2014), which accounts for declining transport efficiency with increasing distance from streams. To roughly calibrate this component of the model to local sediment yields from small catchments (Wagenbrenner & Robichaud, 2014), we doubled the predicted SDR. Sediment was then summed for each catchment and routed down the flowline network to water supply nodes based on a simple channel SDR model (Frickel et al., 1975) adapted to the channel types in the study area to reflect increasing transport efficiency with stream order due to increasing flows and declining roughness. Model evaluation is presented in the Appendix.

Annual sediment load from wildfire was converted to average poststorm SSC in three steps. First, we adjusted our sediment predictions to reflect that approximately 35% of the mass should contribute to the suspended load based on postfire erosion and streamflow monitoring in or near the study region (Ryan, Dwire, & Dixon, 2011; Schmeer, 2014). The average storm suspended sediment load was then calculated by dividing the annual suspended load by the number of sediment-generating storms from the resampled rainfall records. Third, we calculate SSC for the average storm using standard daily load calculations for either the reservoir or stream daily flow volume (Table I) to reflect that, in this region, postfire SSC rises to concerning levels for short peri-

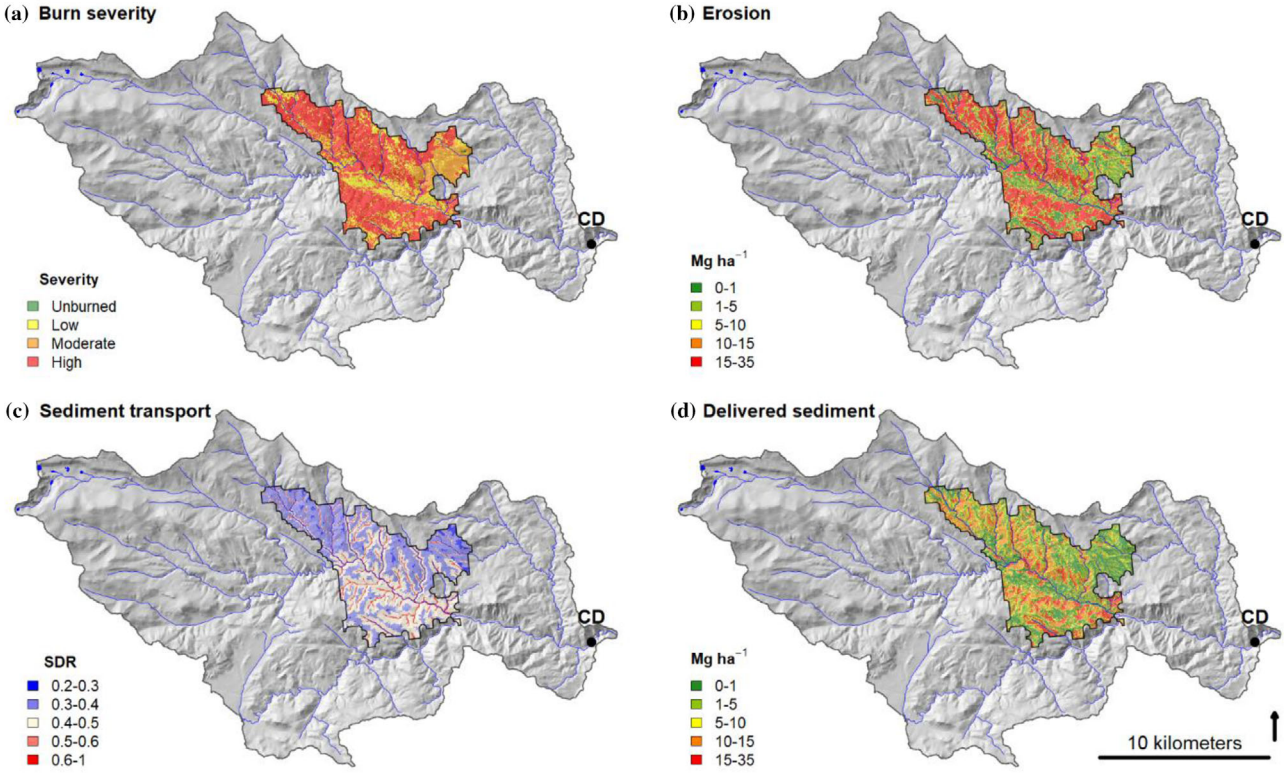

Fig 3. The watershed modeling workflow is demonstrated for a 5,234 ha fire from year 1,610 of the Monte Carlo simulation. Panel A shows the modeled burn severity. Panel B maps the first-year postfire erosion of fine sediments for a rainfall erosivity of 735 MJ mm ha^{-1} h^{-1} from the resampled historical records. Panel C shows the combined hillslope and channel sediment delivery ratio (SDR). Panel D depicts the annual sediment contributed from each pixel to the conveyance diversion. The total postfire sediment load to the diversion in the first-year postfire is 34,689 Mg, which is distributed over six sediment producing storms in the season for an average storm load of 5,781 Mg. For a mean daily flow volume of 4.73×10^8 lpd, the average poststorm SSC is estimated at 12,218 mg/L with an associated turbidity of 10,476 NTU.

ods (hours to days) following rainstorms (Oropeza & Heath, 2013; Sham et al., 2013). Lastly, we convert from SSC (mg/L) to turbidity in nephelometric turbidity units (NTUs) for ease of comparison with water treatment limits using an empirical equation developed from postfire monitoring of a nearby watershed (Equation 1; Murphy et al., 2015).

$$\text{Turbidity} = \frac{\text{SSC} - 2.84}{1.166} \quad (1)$$

2.3. Risk Analysis

For individual infrastructure components, probability of impairment was calculated as the frequency of annual turbidity exceedances over the total number of simulation years. We considered water quality impaired when turbidity exceeded 100 NTU based on recent postfire water operations in the study region (Writer et al., 2014). The wildfire and watershed components of the Monte Carlo simulation (Fig. 2) make reasonable predictions of postfire sediment yields in this region (see Appendix for model evaluation), but the assumptions required to estimate SSC add additional levels of uncertainty. To assess risk metric sensitivity to data and model uncertainties, we also calculate impairment probabilities for 10 NTU and 1,000 NTU impact thresholds assuming the suspended sediment predictions are unlikely to be more than an order of magnitude off in either direction.

To examine system level risks from water quality impairment, we focused on four subsystems that represent examples of redundancy and dependency. For each subsystem, the number of impaired components was tracked on an annual basis and the consequences of impairment were interpreted in light of the subsystem function as follows:

(1) *Redundant sources (TD and TR2)* can meet the dependent community's water demand if

Table II. Frequency of fire by Watershed Area Burned and Conditional Statistics on Annual Area Burned. * Of the Burnable Contributing Area Conditional on Fire Occurrence

Code	Frequency by Watershed Area Burned (% of Years)						Conditional Watershed Area Burned (ha)				
	> 0 ha	> 100 ha	> 1,000 ha	> 10,000 ha	> 20%*	> 50%*	Median	Mean	Max	*SD*	Skew
CR1	0.82	0.24	0.00	0.00	13.41	7.32	27	120	918	202	2.4
CR2	0.33	0.06	0.00	0.00	60.61	54.55	57	48	101	39	0.1
CR3	8.38	2.85	0.89	0.01	1.07	0.00	31	397	12,100	1,124	5.4
CR4	0.94	0.00	0.00	0.00	100.00	100.00	1	1	1	0	NA
CR5	1.92	1.22	0.00	0.00	58.85	39.06	214	327	795	303	0.5
CR6	1.62	1.01	0.00	0.00	59.26	40.74	218	255	615	229	0.4
CD	19.36	8.99	3.96	0.49	1.70	0.05	78	1,147	33,445	3,130	4.9
TD	27.14	10.75	3.89	0.37	0.22	0.00	46	730	31,177	2,313	6.4
TR1	1.21	0.67	0.00	0.00	55.37	30.58	154	227	979	262	1.8
TR2	2.41	1.20	0.48	0.00	24.90	9.54	95	502	3,447	778	1.9

at least one source is operating at full capacity. Therefore, water shortage only occurs if both sources are impaired in the same year.

(2) *Conveyance path 1 (CR1 → CR2 → CR3 → CR4 → CR5 → CR6)* is the primary conveyance path for a regional water project that distributes water to several terminal reservoirs including TR1 and TR2. The conveyance reservoirs were considered nodes at which impaired water may disrupt conveyance.

(3) *Conveyance path 2 (CR1 → CR2 → CR3 → CD)* is an alternative conveyance path that bypasses CR4, CR5, and CR6.

(4) *Redundant conveyance (paths 1 and 2)* provides operational flexibility to deliver water to TR2. System performance was assessed on an annual basis using the least impaired path.

3. RESULTS

3.1. Wildfire Occurrence

A total of 5,741 FSim fires intersected the study watersheds. Including area burned outside the watersheds, their sizes ranged from 2 to 131,922 ha with a median of 59 ha and mean of 1,758 ha. The low to mid elevations are predicted to burn more frequently than the high elevations owing to variation in fuels and climate (Fig. 1). The area just upstream of TD has low predicted burn probability because fuels were recently reduced by wildfire. Wildfire is predicted to occur most frequently and to impact the greatest area in the large watersheds associated with the on-network diversions—CD and TD (Fig. 1; Table II). Wildfires occurred in 19.4% of years in the CD watershed and 27.1% of years in the TD watershed. The other on-network water supply, CR3, was exposed to much less wildfire activity because of its smaller watershed and the lower frequency of burning at higher elevations (Fig. 1; Table II). Predicted wildfire activity is low in the local contributing areas to the off-network reservoirs (Table II). TR2 was the most-frequently exposed off-network water supply (2.4% of years), because of its moderate contributing area and low elevation. Only four water supplies—CR3, CD, TD, and TR2—were exposed to more than 1,000 ha fire in single year. Greater than 10,000 ha of annual fire activity was only observed for the three on-network water supplies—CR3, CD, and TD—and this level of burning was very rare (Table II). Only CD and TD experienced greater than 30,000 ha burned in a year. Although off-network water supplies were rarely exposed to fire, proportionally more of their watersheds were affected when they did burn (Table II).

3.2. Burn Severity and Suspended Sediment

Fire effects on water supplies are predicted to differ considerably across the study area due to variability in fuels and topography that influence burn severity, soils, and topography that affect hillslope erosion, and proximity to water supplies that controls sediment transport efficiency (Fig. 4). Low, moderate, and high severity burning is predicted to occur on 24.4%, 16.5%, and 44.4% of the study area, respectively. The remaining 14.7% of the study area is nonburnable cover (barren alpine, water, urban, etc.). Watershed area burned at moderate and high severity ranged between 38.6% to 78.6% by water supply.

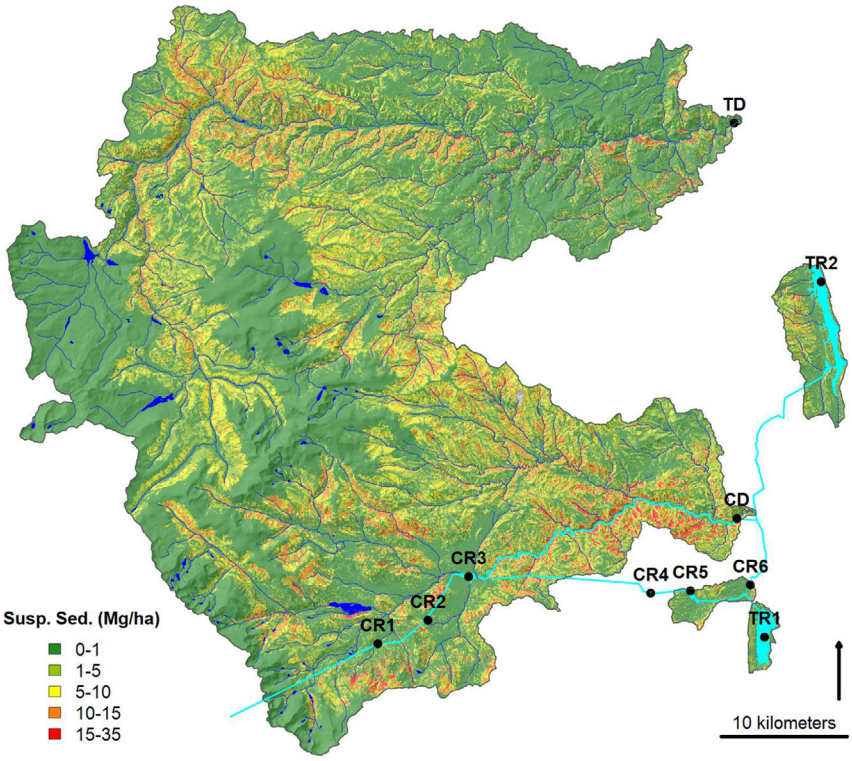

Fig 4. Predicted contribution of suspended sediment to water supplies during the first-year postfire under median annual rainfall erosivity (403 MJ mm ha^{-1} h^{-1}). The major conveyance paths and reservoirs are cyan.

For median May through October rainfall erosivity (403 MJ mm ha^{-1} h^{-1}), fire is predicted to increase erosion between 0 and 100 Mg/ha with a mean of 23.0 Mg/ha and a standard deviation of 32.0 Mg/ha. The associated mean production of fine sediments contributing to the suspended load is 8.1 Mg/ha. A substantial portion of the eroded sediment is retained on hillslopes, so the mean fine sediment delivery to streams is only 4.0 Mg/ha with a standard deviation of 5.8 Mg/ha. Retention in channels further reduces the average contribution to water supplies to a mean of 2.6 Mg/ha with a standard deviation of 4.1 Mg/ha. Much of the channel transport losses are from reservoirs and lakes that reduce downstream connectivity (Fig. 4).

3.3. Water Supply Exposure to Suspended Sediment

The Monte Carlo simulation linked time and location varying wildfire occurrence and time varying rainfall to predict the annual average poststorm SSC from all wildfire activity accounting for recovery for the first three postfire years (Fig. 2). Fig. 5 illustrates a 500-year subset of the simulation for TD. Wildfire was frequent in the watershed due to its large size, but not all wildfire resulted in problematic SSC, either because it did not affect enough area or because it did not align with high rainfall erosivity. Within this subset of the simulation, 50 years had greater than 100 ha of wildfire activity resulting in 79 years that turbidity exceeded the 100 NTU impairment threshold. Impairment was more frequent than large fire occurrence because burned areas are susceptible to erosion for multiple years.

Cumulative frequency distributions of annual average poststorm turbidity for the full 10,000 year simulation period are shown for each of the water supplies in Fig. 6. Mean poststorm turbidity, conditional on fire occurrence, varied from 2 to 2,129 NTU for reservoirs and from 381 to 2,943 NTU for diversions. Turbidity only exceeded 1,000 NTU in 5% or more of the fire-affected years at CR1, CD, and TD. The on-network diversions were most frequently impaired; poststorm turbidity at CD and TD exceeded 100 NTU in 19.35% and 15.74% of years, respectively. The one on-network reservoir—CR3—was impaired in 2.76% of years. Off-network reservoirs were rarely impaired (Fig. 6); the most frequently impaired reservoir only exceeded 100 NTU in 1.67% of simulation years. Two reservoirs—CR4 and TR1—were never impaired and TR2 was only impaired once in 10,000 years.

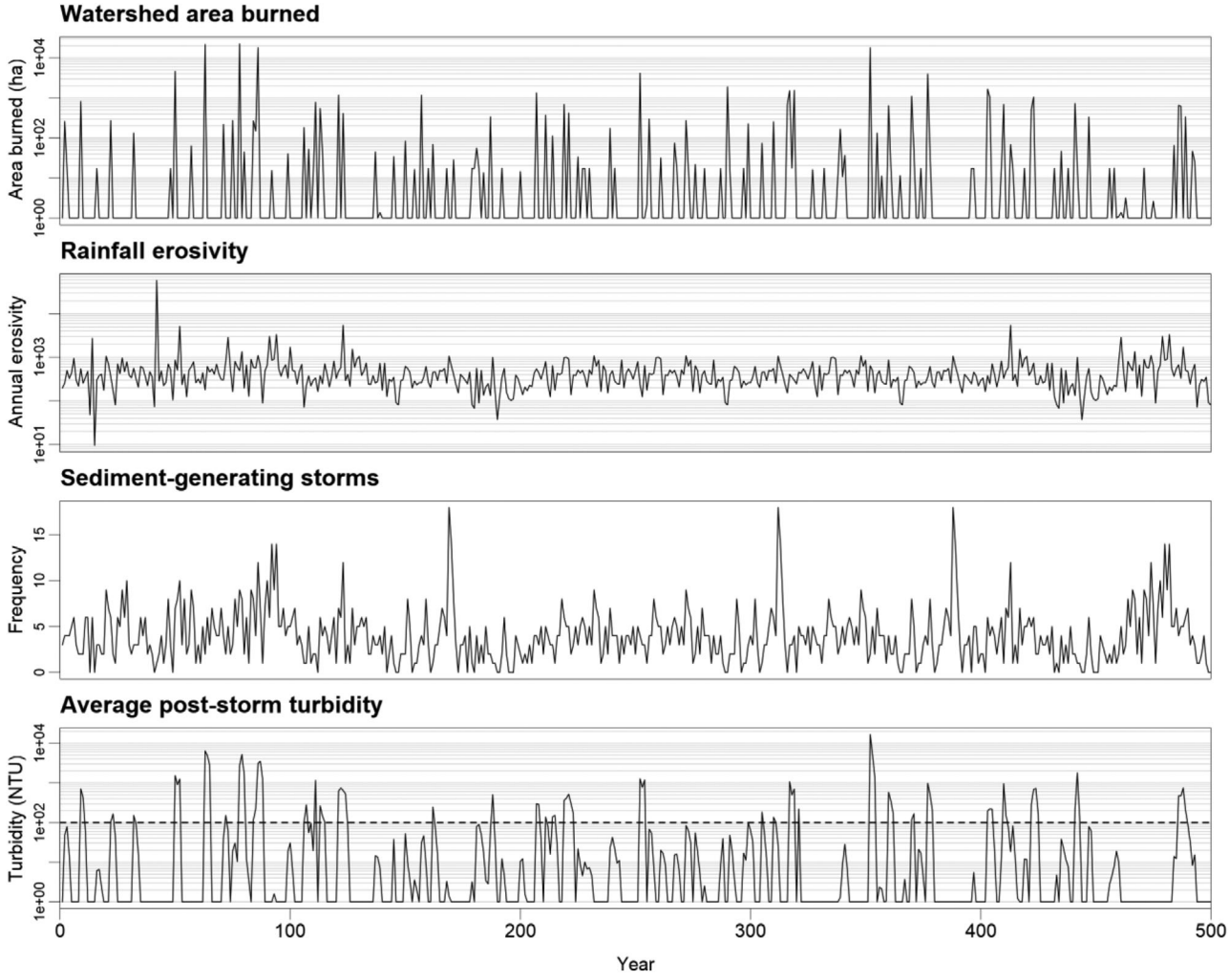

Fig 5. An example 500-year subset of the Monte Carlo simulation for the terminal diversion (TD) showing annual watershed area burned, rainfall erosivity, number of sediment-generating storms, and average post storm turbidity. The dashed horizontal line marks the 100 NTU impairment threshold. The 100 NTU exceedance probability for this subset of the simulation is 0.158.

Table III. Frequency of Impaired Components by Subsystem and NTU Impact Threshold

Scenario	NTU	Impaired Components (% of Years)								
		0	1	2	3	4	5	6	≥ 1	≥ 2
Redundant sources	10	68.50	31.44	0.06	NA	NA	NA	NA	31.50	0.06
	100	84.26	15.73	0.01	NA	NA	NA	NA	15.74	0.01
	1000	95.77	4.23	0.00	NA	NA	NA	NA	4.23	0.00
Conveyance path 1	10	88.15	8.38	2.57	0.71	0.15	0.04	0.00	11.85	3.47
	100	94.83	4.21	0.86	0.09	0.01	0.00	0.00	5.17	0.96
	1000	99.05	0.84	0.11	0.00	0.00	0.00	0.00	0.95	0.11
Conveyance path 2	10	67.86	25.67	5.27	0.98	0.22	NA	NA	32.14	6.47
	100	79.03	18.56	1.96	0.42	0.03	NA	NA	20.97	2.41
	1000	89.17	10.52	0.22	0.09	0.00	NA	NA	10.83	0.31
Redundant conveyance	10	88.84	9.23	1.52	0.37	0.04	0.00	0.00	11.16	1.93
	100	95.05	4.23	0.65	0.07	0.00	0.00	0.00	4.95	0.72
	1000	99.05	0.84	0.11	0.00	0.00	0.00	0.00	0.95	0.11

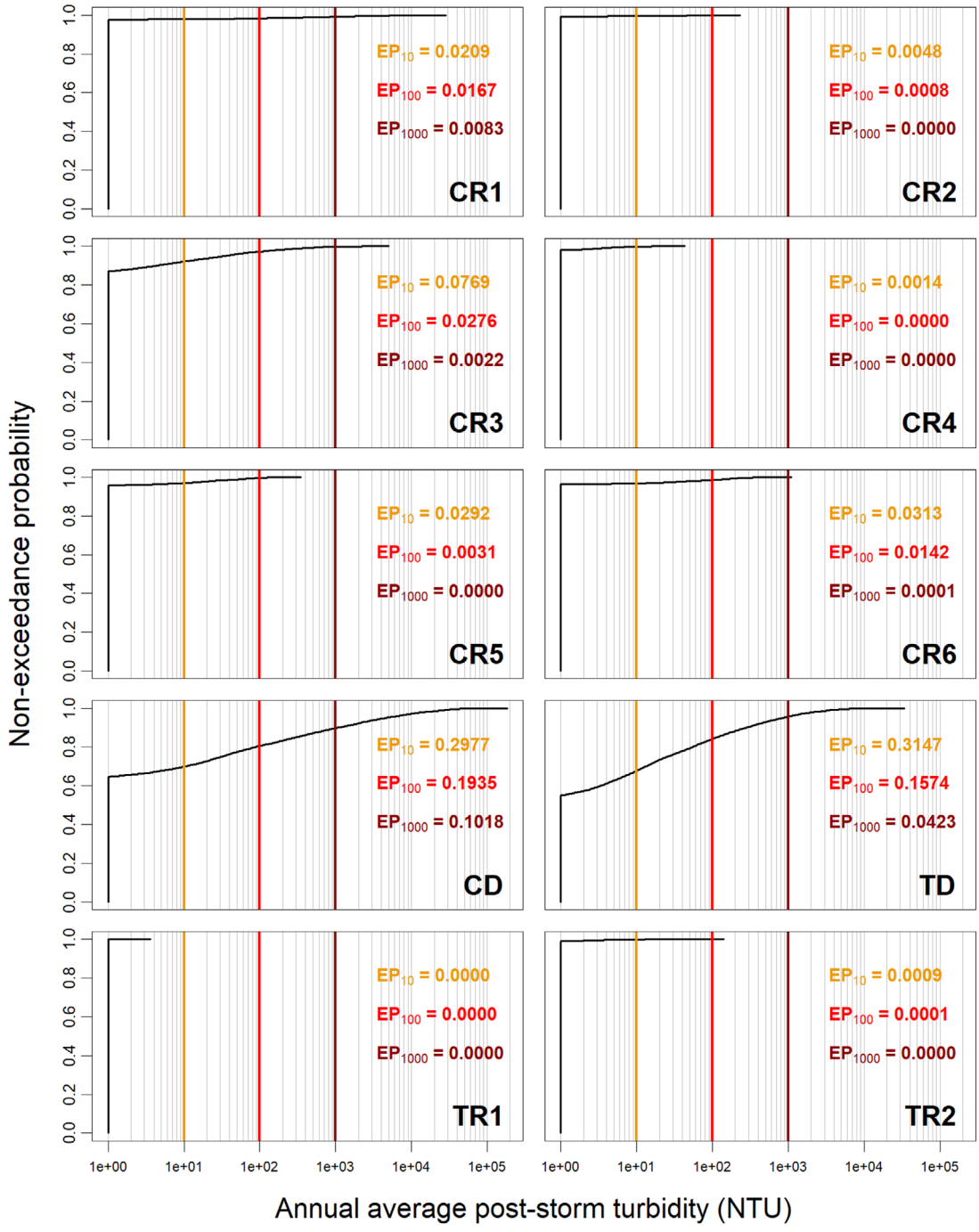

Fig 6. Cumulative frequency distributions of annual average poststorm turbidity by water supply with 10, 100, and 1,000 NTU exceedance probabilities (EP).

3.4. System-level Consequences

The frequency of component impairment is presented by subsystem and turbidity impairment threshold in Table III. The redundant sources subsystem experienced at least one component impairment in 15.74% of years, but coimpairment of the dual sources only occurred once in 10,000 years. Accounting for this redundancy decreased the

risk of water supply disruption by 99.9% compared to the naïve assumption of disruption whenever a single component is impaired. In contrast, dependency magnified risk. CR3 was the most frequently impaired component on conveyance path 1 at 2.76% of years, but at least one component was impaired along the path in 5.17% of years. The multiple nodes of impact increased exposure to wildfire risk. If two or more impaired components are required to substantially reduce annual water conveyance, conveyance route 1 only experienced disruption in 0.96% of years. Conveyance path 2 was much risker due to the frequent impairment of CD (Fig. 6). One or more components of conveyance path 2 were impaired in 20.97% of years and two or more components were impaired in 2.41% of years. Despite the low reliability of conveyance path 2, it provided some level of redundancy for path 1. The redundant conveyance scenario reduced the frequency of at least one impairment from 5.17% to 4.95% of years (a 4.3% reduction) and it reduced the frequency of at least two impairments from 0.96% to 0.72% of years (a 25.0% reduction).

4. DISCUSSION

This work demonstrates the importance of considering water system characteristics when assessing wildfire risk to water supplies. The Monte Carlo simulation included realistic representations of wildfire and rainfall activity, postfire watershed response, and water supply sensitivity to sediment to estimate the probability of water impairment. Our results suggest that water supplies with large contributing areas are most at risk of impairment due to their frequent exposure to wildfires large enough to mobilize problematic sediment quantities. Off-network water supplies are at lower risk because wildfire is less likely to encounter small watersheds. Larger waterbodies are also more resistant to impairment due their greater capacity to dilute contaminants. Hence, large off-network reservoirs are at very low risk of impairment. The results also demonstrate that risk of system disruption is reduced by redundancy and magnified by dependency. Our test scenarios show how disruption risk can be lowered with both highly reliable large off-network reservoirs and alternative conveyance routes. In contrast, conveyance systems with multiple nodes of impact may magnify risk because it is more likely that fire will encounter their collective watershed areas.

This study builds upon previous applications of Monte Carlo wildfire simulation to assess water supply risk by linking stochastic wildfire and rainfall activity with realistic models of watershed response and water supply sensitivity to impairment. The wide range of wildfire and rainfall magnitudes (Fig. 5) combine to produce substantial variation in watershed effects (Fig. 6) similar to the results of earlier studies in California, Colorado, and New Mexico (Buckley et al., 2014; Haas et al., 2017; Thompson et al., 2016). Watershed response is also considerably influenced by the location and pattern of wildfire activity relative to spatial variation in the biophysical drivers of fire behavior, postfire erosion, and sediment transport (Fig. 4). Our predictions of postfire suspended sediment yields are within the 0 to 50 Mg ha^{-1} yr^{-1} reported by previous studies (Smith et al., 2011) and most of our poststorm turbidities are in the common range of 100–1,000 NTU reported after wildfires in the study region (Fig. 6; Murphy et al., 2015; Oropeza & Heath, 2013; Rhoades, Entwistle, & Butler, 2011). Postfire sediment production from montane watersheds in southwest and pacific northwest regions of the United States should be similar or slightly higher than predicted here (Moody & Martin, 2009). Characterizing impairment in terms of operational turbidity limits provides an objective means to define what combination of wildfire and rainfall magnitudes are problematic. A key result of our analysis is that much of the wildfire and rainfall activity, especially in the larger watersheds, did not result in impairment (Fig. 6); for example, TD only exceeded 100 NTU in 35.0% of the years that it was exposed to wildfire sediment. Further analysis of fire and rainfall characteristics associated with impairment may help managers better understand and mitigate risk.

The limitations of linked fire and watershed models have been discussed extensively in prior publications (e.g., Elliot et al., 2016; Gannon et al., 2019; Jones et al., 2017), but it is worth reiterating that coupling diverse data sources and models has potential for prediction error due to data, model, and model linkage uncertainties. A limitation of the fire modeling in this study is the use of current fuel conditions and historical climate to model both wildfire occurrence and severity, which does not account for the impacts of climate change and vegetation dynamics on future fire activity. The watershed modeling in this study also has several limitations. We used the average annual storm sediment load to gage water supply impacts instead of modeling sediment load from individual storms. We also did not account for the

potential cumulative impact of closely timed storms on SSC. The assumption that the sediment load is equally mixed in the average annual reservoir or daily flow volume is also an approximation. Rainfall was treated as a spatially uniform process, but highly localized and intense rainstorms are the norm in this region (Kampf et al., 2016; Moody & Martin, 2009; Murphy et al., 2015). Incorporating spatial variability in rainfall might further reduce risk to water supplies with small watersheds because the probability of encountering intense rainfall should be lower than for large watersheds. The use of turbidity as a single metric of water quality is a reasonable simplification in our study region based on the documented impacts of past wildfires (Sham et al., 2013), but elevated carbon, nutrients, and heavy metals also have the potential to impair water quality (Abraham et al., 2017; Emelko, Silins, Bladon, & Stone, 2011; Smith et al., 2011). Assessing impairment risk from other contaminants may require different watershed modeling because the factors that influence the magnitude and timing of their postfire concentrations vary (Rust et al., 2019) due to differences in contaminant sources, mobilization, and transport. The sediment-centric approach used here should be relevant to other steep montane watersheds, but it is less applicable to low-relief landscapes with minor postfire erosion (e.g., boreal forest).

The annual impairment probabilities modeled in this study for individual water supplies span the range of 0–0.1935 at a 100 NTU standard. The on-network diversions—CD and TD—had the highest probability of impairment at 0.1574 and 0.1935, respectively. Given that fire often impairs water for two years, this corresponds to an impactful wildfire on average once every 10–13 years. Our estimated impairment probability of 0.0276 for the one on-network reservoir—CR3—is close to the prediction that SSC will exceed problematic levels every 18–124 years in a reservoir with a similar sized watershed in Australia (Langhans et al., 2016). Previous work suggests water supplies from small watersheds may be more prone to impairment due to the greater conditional probability of burning a high proportion of the area (Thompson, Scott, Kaiden et al., 2013) and the smaller flows to dilute contaminants (Robinne et al., 2019). In contrast, the water supplies with the smallest watersheds in this study—the off-network reservoirs—had the lowest probability of impairment because their watersheds rarely burned (Table II) and their large volumes lowered their sensitivity to sediment. Large reservoirs with small contributing areas, similar to TR1 and TR2 in this study, should be at very low risk of impairment, but we suspect that large reservoirs with large watersheds, such as those in California (Buckley et al., 2014), have impairment probabilities closer to CD and TD in this study due to their similar watershed sizes and erosion potential.

Increasing source water redundancy is often advocated for as a means to mitigate wildfire-water supply risks (Martin, 2016; Murphy et al., 2015; Sham et al., 2013), but without quantitative estimates of the mitigation benefit. Covariance in fire exposure across a multisource water system has been proposed as a means to optimize mitigation decisions using a portfolio investment framework (Warziniack & Thompson, 2013). The Monte Carlo simulation methods used here allowed for meaningful characterization of the likelihood that multiple system components will be impaired at the same time (Table III). Our results illustrate two forms of redundancy that are common in many water systems. The first is mitigating uncertainty with a high reliability water source, in this case, a large off-network terminal reservoir. Assuming 100% substitutability, TR2 reduced the risk of water supply disruption to practically zero despite frequent impairment to TD (Table III). The second form of redundancy reduces risk of water shortage through alternative conveyance paths. The alternative conveyance paths in this study provided some disruption protection despite their close proximity and the low reliability of path 2. The gain in system reliability from alternative sources and conveyance pathways should increase with geographic separation.

Wildfire risk magnification from dependencies has not been widely discussed. For conveyance path 1, we found modest risk magnification from the dependent nature of conveyance infrastructure; the most frequently impacted component was impaired 2.76% of simulation years but at least one component on the conveyance path was impaired in 5.17% of years. This increase is a result of the larger watershed area exposed to wildfire. For this assessment, it was assumed the 100 NTU impairment threshold for water treatment also applies to conveyance due to the undesirable effects of sedimentation to intake structures, pipelines, and canals, but it is possible that these components are less sensitive to suspended sediment and therefore the absolute risk is lower. Future assessments of conveyance disruption would benefit from incorporating more information on the operational constraints. Still, the magnification we ob-

served approximately doubled the likelihood of a conveyance disruption, which highlights the importance of considering cumulative exposure for dependent systems.

The results of this study have several implications for management. The most obvious are that water supply reliability should improve by reducing wildfire exposure and adding redundancies. Whenever possible, reservoirs should be situated in off-network locations with small contributing areas and nodes of impact along conveyance routes should be avoided to reduce exposure. This study demonstrates that some water systems may already have low disruption risk due to existing source water redundancies, but communities that rely heavily on a single reservoir or diversion from a fire prone watershed should consider developing alternative sources in watersheds that are unlikely to burn at the same time as their primary source. Given the difficulty of modifying infrastructure systems and acquiring new water sources, there has been considerable interest in alternative mitigation options such as improved fire containment (Haas et al., 2017), reducing fuels in source watersheds (Elliot et al., 2016; Gannon et al., 2019), postfire erosion control (Robichaud, Lewis, et al., 2013; Schmeer, Kampf, MacDonald, Hewitt, & Wilson, 2018; Wagenbrenner et al., 2006), improved monitoring to utilize water between impairment events (Martin, 2016), and constructing basins to remove sediment before sensitive conveyance or treatment infrastructure (Writer et al., 2014). The effectiveness and feasibility of these solutions are likely to vary by community based on watershed and infrastructure characteristics. The risk analysis methods presented this study could be adapted to evaluate the effectiveness of alternative mitigation strategies at reducing impairment and system disruption risks.

5. CONCLUSION

Monte Carlo simulation of water quality in response to stochastic wildfire and rainfall forcings provides a means to account for scale-dependent effects in wildfire-water supply risk assessment. Our results suggest that the off-network reservoirs in our study system are at low risk of impairment because wildfire will rarely encounter their small watersheds and their large volumes can dilute many postfire sediment loads below the concentration threshold for impairment. In contrast, diversions from the largest watersheds were found to be at high risk of impairment due to their greater exposure to large wildfires. At the system level, disruption risk was dramatically reduced by redundancy and nearly doubled by dependency. These results highlight the importance of accounting for operational constraints and functional relationships between infrastructure when assessing risk of disrupting multisource water systems. Our results also validate that previous recommendations to develop alternative water sources should meaningfully increase water supply reliability, especially when one of them is at low risk of impairment. Dependencies among system components should also be avoided so as not to magnify wildfire risk by increasing exposure.

ACKNOWLEDGMENTS

The authors thank Codie Wilson for sharing the rainfall data used in the analysis. The work presented in this article builds on prior research and applied projects funded by joint venture agreement number 19-JV-11221636-170 between USDA Forest Service Rocky Mountain Research Station and Colorado State University and agreement number 19-DG-11031600-062 between USDA Forest Service Southwestern Region and the Colorado Forest Restoration Institute at Colorado State University.

REFERENCES

Abraham, J., Dowling, K., & Florentine, S. (2017). Risk of postfire metal mobilization into surface water resources: A review. *Science of the Total Environment*, *599–600*, 1740–1755. https://doi.org/10.1016/j.scitotenv.2017.05.096

Benavides-Solorio, J. D., & MacDonald, L. H. (2005). Measurement and prediction of post-fire erosion at the hillslope scale, Colorado Front Range. *International Journal of Wildland Fire*, *14*, 457–474. https://doi.org/10.1071/WF05042

Bradshaw, L., & McCormick, E. (2000). *FireFamily plus user's guide (version 2.0)*. (General Technical Report RMRS-GTR-67WWW). Ogden, UT: USDA Forest Service, Rocky Mountain Research Station.

Buckley, M., Beck, N., Bowden, P., Miller, M. E., Hill, B., Luce, C., … Gaither, J. (2014). *Mokelumne watershed avoided cost analysis: Why Sierra fuel treatments make economic sense*, Auburn, CA: Sierra Nevada Conservancy.

Crosby, J. S., & Chandler, C. C. (1966). Get the most from your windspeed observation. *Fire Control Notes*, *27*, 12–13.

Elliot, W. J., Miller, M. E., & Enstice, N. (2016). Targeting forest management through fire and erosion modelling. *International Journal of Wildland Fire*, *25*, 876–887. https://doi.org/10.1071/WF15007

Emelko, M. B., Silins, U., Bladon, K. D., & Stone, M. (2011). Implications of land disturbance on drinking water treatability in a changing climate: Demonstrating the need for "source water supply and protection" strategies. *Water Research*, *45*, 461–472. https://doi.org/10.1016/j.watres.2010.08.051

ESRI (2015). *ArcGIS (version 10.3)*. Redlands, CA: Environmental Systems Research Institute.

Finney, M. A. (2002). Fire growth using minimum travel time methods. *Canadian Journal of Forest Research*, *32*(8), 1420–1424. https://doi.org/10.1139/x02-068

Finney, M., Grenfell, I. C., & McHugh, C. W. (2009). Modeling containment of large wildfires using generalized linear mixed-model analysis. *Forest Science*, *55*, 249–255.

Finney, M. A., McHugh, C. W., Grenfell, I. C., Riley, K. L., & Short, K. C. (2011). A simulation of probabilistic wildfire risk components for the continental United States. *Stochastic Environmental Research and Risk Assessment*, *25*, 973–1000. https://doi.org/10.1007/s00477-011-0462-z

Finney, M. A., Brittain, S., Seli, R. C., McHugh, C. W., & Gangi, L. (2015). *FlamMap: Fire mapping and analysis system (version 5.0)*. Missoula, MT: USDA Forest Service, Rocky Mountain Research Station, Fire Lab.

Frickel, D. G., Shown, L. M., & Patton, P. C. (1975). *An evaluation of hillslope and channel erosion related to oil-shale development in the Piceance basin, north-western Colorado*. Colorado Water Resources Circular 30. Denver, CO: Colorado Department of Natural Resources.

Gannon, B. M., Wei, Y., MacDonald, L. H., Kampf, S. K., Jones, K. W., Cannon, J. B., … Thompson, M. P. (2019). Prioritising fuels reduction for water supply protection. *International Journal of Wildland Fire*, *28*, 785–803. https://doi.org/10.1071/WF18182

Graham, R. T. (2003). *Hayman Fire case study*. General Technical Report RMRS-GTR-114. Ogden, UT: USDA Forest Service, Rocky Mountain Research Station.

Haas, J. R., Thompson, M., Tillery, A., & Scott, J. H. (2017). Capturing spatiotemporal variation in wildfires for improving post-wildfire debris-flow hazard assessments. In K. Riley, P. Webley, & M. Thompson (Eds.), *Natural hazard uncertainty assessment: Modeling and decision support, geophysical monograph 223* (pp. 301–317). Hoboken, NJ: John Wiley & Sons.

Haimes, Y. Y. (2012). Systems-based guiding principles for risk modeling, planning, assessment, management, and communication. *Risk Analysis*, *32*(9), 1451–1467. https://doi.org/10.1111/j.1539-6924.2012.01809.x

Hallema, D. W., Kinoshita, A. M., Martin, D. A., Robinne, F.-N., Galleguillos, M., NcNulty, S. G., … Moore, P. F. (2019). Fire, forests and city water supplies. *Unasylva*, *70*(1), 58–66.

Henkle, J. E., Wohl, E., & Beckman, N. (2011). Locations of channel heads in the semiarid Colorado Front Range, USA. *Geomorphology*, *129*, 309–319. https://doi.org/10.1016/j.geomorph.2011.02.026

Jones, O. D., Nyman, P., & Sheridan, G. J. (2014). Modelling the effects of fire and rainfall regimes on extreme erosion events in forested landscapes. *Stochastic Environmental Research and Risk Assessment*, *28*, 2015–2025. https://doi.org/10.1007/s00477-014-0891-6

Jones, K. W., Cannon, J. B., Saavedra, F. A., Kampf, S. K., Addington, R. N., Cheng, A. S., … Wolk, B. (2017). Return on investment from fuel treatments to reduce severe wildfire and erosion in a watershed investment program in Colorado. *Journal of Environmental Management*, *198*, 66–77. https://doi.org/10.1016/j.jenvman.2017.05.023

Kampf, S. K., Brogan, D. J., Schmeer, S., MacDonald, L. H., & Nelson, P. A. (2016). How do geomorphic effects of rainfall vary with storm type and spatial scale in a post-fire landscape? *Geomorphology*, *273*, 39–51. https://doi.org/10.1016/j.geomorph.2016.08.001

LANDFIRE (2016). *Fuel, topography, existing vegetation type, and fuel disturbance layers (Version 1.4.0)*. Washington, DC: US Geological Survey.

Langhans, C., Smith, H. G., Chong, D. M. O., Nyman, P., Lane, P. N. J., & Sheridan, G. J. (2016). A model for assessing water quality risk in catchments prone to wildfire. *Journal of Hydrology*, *534*, 407–426. https://doi.org/10.1016/j.jhydrol.2015.12.048

Larsen, I. J., & MacDonald, L. H. (2007). Predicting post-fire sediment yields at the hillslope scale: Testing RUSLE and disturbed WEPP. *Water Resources Research*, *43*, W11412. https://doi.org/10.1029/2006WR005560

Larsen, I. J., MacDonald, L. H., Brown, E., Rough, D., Welsh, M. J., Pietraszek, J. H., … Schaffrath, K. (2009). Causes of post-fire runoff and erosion: Water repellency, cover, or soil sealing? *Soil Science Society of America Journal*, *73*, 1393–1407. https://doi.org/10.2136/sssaj2007.0432

Martin, D. A. (2016). At the nexus of fire, water and society. *Philosophical Transactions of the Royal Society of London. Series B, Biological Sciences*, *371*, 20150172. https://doi.org/10.1098/rstb.2015.0172

Miller, S., Rhodes, C., Robichaud, P., Ryan, S., Kovecses, J., Chambers, C., … Rocca, M. (2017). *Learn from the burn: The High Park fire 5 years later*. Science You Can Use Bulletin, Issue 25. Fort Collins, CO: USDA Forest Service, Rocky Mountain Research Station.

Moody, J. A., & Martin, D. A. (2001). Initial hydrologic and geomorphic response following a wildfire in the Colorado Front Range. *Earth Surface Processes and Landforms*, *26*, 1049–1070. https://doi.org/10.1002/esp.253

Moody, J. A., & Martin, D. A. (2009). Synthesis of sediment yields after wildland fire in different rainfall regimes in the western United States. *International Journal of Wildland Fire*, *18*, 96–115. https://doi.org/10.1071/WF07162

Moore, C., Kampf, S., Stone, B., & Richer, E. (2015). A GIS-based method for defining snow zones: Application to the western United States. *Geocarto International*, *30*(1), 62–81. https://doi.org/10.1080/10106049.2014.885089

Murphy, S. F., Writer, J. H., McCleskey, R. B., & Martin, D. A. (2015). The role of precipitation type, intensity, and spatial distribution in source water quality after wildfire. *Environmental Research Letters*, *10*, 084007. https://doi.org/10.1088/1748-9326/10/8/084007

NRCS Soil Survey Staff (2016). *Web soil survey*. Washington, DC: USDA Natural Resources Conservation Service. Retrieved from https://websoilsurvey.nrcs.usda.gov/

Nunes, J. P., Doerr, S. H., Sheridan, G., Neris, J., Santín, C., Emelko, M. B., … Keizer, J. (2018). Assessing water contamination risk from vegetation fires: Challenges, opportunities and a framework for progress. *Hydrological Processes*, *32*, 687–694. https://doi.org/10.1002/hyp.11434

Oropeza, J., & Heath, J. (2013). *Effects of the 2012 Hewlett and High Park wildfires on water quality of the Poudre River and Seaman Reservoir*. Fort Collins, CO: City of Fort Collins Utilities.

Perica, S., Martin, D., Pavlovic, S., Roy, I., St Laurent, M., Trypaluk, C., … Bonnin, G. (2013). *NOAA Atlas 14, Volume 8, precipitation-frequency atlas of the United States, Midwestern States (Version 2)*, Silver Springs, MD: US National Oceanic and Atmospheric Administration.

Pietraszek, J. H. (2006). *Controls on post-fire erosion at the hillslope scale, Colorado Front Range*. (Unpublished MS Thesis). Colorado State University, Fort Collins, CO.

PRISM (2014). *Annual precipitation normals (Version 14.1)*, Corvallis, OR: PRISM Climate Group, Oregon State University. Retrieved from http://prism.oregonstate.edu

Renard, K. G., Foster, G. R., Weesies, G. A., McCool, D. K., & Yoder, D. C. (1997). *Predicting soil erosion by water: A guide to conservation planning with the Revised Universal Soil Loss Equation (RUSLE)*. Agricultural Handbook no. 703. Washington, DC: USDA Agricultural Research Service.

Rhoades, C. C., Entwistle, D., & Butler, D. (2011). The influence of wildfire extent and severity on streamwater chemistry, sediment and temperature following the Hayman Fire, Colorado. *International Journal of Wildland Fire*, *20*, 430–442. https://doi.org/10.1071/WF09086

Rhoades, C. C., Nunes, J. P., Silins, U., & Doerr, S. H. (2019). The influence of wildfire on water quality and watershed processes: New insights and remaining challenges. *International Journal of Wildland Fire*, *28*, 721–725. https://doi.org/10.1071/WFv28n10_FO

Robichaud, P. R., Wagenbrenner, J. W., Brown, R. E., Wohlgemuth, P. M., & Beyers, J. L. (2008). Evaluating the effectiveness of contour-felled log erosion barriers as a post-fire runoff and erosion mitigation treatment in the western United States. *International Journal of Wildland Fire*, *17*, 255–273. https://doi.org/10.1071/WF07032

Robichaud, P. R., Lewis, S. A., Wagenbrenner, J. W., Ashmun, L. E., & Brown, R. E. (2013). Post-fire mulching for runoff and erosion mitigation. Part I: Effectiveness at reducing hillslope erosion rates. *Catena*, *105*, 75–92. https://doi.org/10.1016/j.catena.2012.11.015

Robichaud, P. R., Wagenbrenner, J. W., Lewis, S. A., Ashmun, L. E., Brown, R. E., & Wohlgemuth, P. M. (2013). Post-fire mulching for runoff and erosion mitigation. Part II: Effectiveness in reducing runoff and sediment yields from small catchments. *Catena*, *105*, 93–111. https://doi.org/10.1016/j.catena.2012.11.016

Robinne, F.-N., Bladon, K. D., Miller, C., Parisien, M.-A., Mathieu, J., & Flannigan, M. D. (2018). A spatial evaluation of global wildfire-water risks to human and natural systems. *Science of the Total Environment*, *610–611*, 1193–1206. http://doi.org/10.1016/j.scitotenv.2017.08.112

Robinne, F.-N., Bladon, K. D., Silins, U., Emelko, M. B., Flannigan, M. D., Parisien, M.-A., … Dupont, D. P. (2019). A regional-scale index for assessing the exposure of drinking-water sources to wildfires. *Forests*, *10*, 384. https://doi.org/10.3390/f10050384

Rust, A. J., Saxe, S., McCray, J., Rhoades, C. C., & Hogue, T. S. (2019). Evaluating the factors responsible for post-fire water quality response in forests of the western USA. *International Journal of Wildland Fire*, *28*(10), 769–784. https://doi.org/10.1071/WF18191

Ryan, S. E., Dwire, K. A., & Dixon, M. K. (2011). Impacts of wildfire on runoff and sediment loads at Little Granite Creek, western Wyoming. *Geomorphology*, *129*, 113–130. https://doi.org/10.1016/j.geomorph.2011.01.017

Sankey, J. B., Kreitler, J., Hawbaker, T. J., McVay, J. L., Miller, M. E., Mueller, E. R., … Sankey, T. T. (2017). Climate, wildfire, and erosion ensemble foretells more sediment in western USA watersheds. *Geophysical Research Letters*, *44*, 8884–8892. https://doi.org/10.1002/2017GL073979

Schmeer, S. R. (2014). Post-fire erosion response and recovery, High Park Fire, Colorado. (Unpublished MS Thesis). Colorado State University, Fort Collins, CO, USA.

Schmeer, S. R., Kampf, S. K., MacDonald, L. H., Hewitt, J., & Wilson, C. (2018). Empirical models of annual post-fire erosion on mulched and unmulched hillslopes. *Catena*, *163*, 276–287. https://doi.org/10.1016/j.catena.2017.12.029

Scott, J. H., & Reinhardt, E. D. (2001). *Assessing crown fire potential by linking models of surface and crown fire behavior*. Research Paper RMRS-RP-29. Fort Collins, CO: USDA Forest Service, Rocky Mountain Research Station.

Shakesby, R. A., & Doerr, S. H. (2006). Wildfire as a hydrological and geomorphological agent. *Earth-Science Reviews*, *74*, 269–307. https://doi.org/10.1016/j.earscirev.2005.10.006

Sham, C. H., Tuccillo, M. E., & Rooke, J. (2013). *Effects of wildfire on drinking water utilities and best practices for wildfire risk reduction and mitigation*. Report 4482. Denver, CO: Water Research Foundation. Retrieved from www.waterrf.org

Short, K. C., Finney, M. A., Scott, J. H., Gilbertson-Day, J. W., & Grenfell, I. C. (2016). *Spatial dataset of probabilistic wildfire risk components for the conterminous United States*. Fort Collins, CO: USDA Forest Service. Research Data Archive. https://doi.org/10.2737/RDS-2016-0034

Singh, V. P., Jain, S. K., & Tyagi, A. (2007). *Risk and reliability analysis: A handbook for civil and environmental engineers*. Reston, VA: American Society of Civil Engineers Press. https://doi.org/10.1061/9780784408919

Smith, H. G., Sheridan, G. J., Lane, P. N. J., Nyman, P., & Haydon, S. (2011). Wildfire effects on water quality in forest catchments: A review with implications for water supply. *Journal of Hydrology*, *396*, 170–192. https://doi.org.j.jhydrol.2010.10.043

Theobald, D. M., Merritt, D. M., & Norman, J. B. (2010). *Assessment of threats to riparian ecosystems in the western U.S.*, Fort Collins, CO: USDA Stream Systems Technology Center and Colorado State University.

Thompson, M. P., Scott, J., Kaiden, J. D., & Gilbertson-Day, J. W. (2013). A polygon-based modeling approach to assess exposure of resources and assets to wildfire. *Natural Hazards*, *67*, 627–644. https://doi.org/10.1007/s11069-013-0593-2

Thompson, M. P., Scott, J., Langowski, P. G., Gilbertson-Day, J. W., Haas, J. R., & Bowne, E. M. (2013). Assessing watershed -wildfire risks on national forest system lands in the Rocky Mountain region of the United States. *Water*, *5*, 945–971. https://doi.org/10.3390/w5030945

Thompson, M. P., Gilbertson-Day, J. W., & Scott, J. H. (2016). Integrating pixel- and polygon-based approaches to wildfire risk assessment: Applications to a high-value watershed on the Pike and San Isabel National Forests, Colorado, USA. *Environmental Modeling and Assessment*, *21*, 1–15. https://doi.org/10.1007/s10666-015-9469-z

Tillery, A. C., Haas, J. R., Miller, L. W., Scott, J. H., & Thompson, M. P. (2014). *Potential post-wildfire debris-flow hazards - a pre-wildfire evaluation for the Sandia and Manzano Mountains and surrounding areas, central New Mexico*. Scientific Investigations Report 2014–5161. Albuquerque, NM: US Geological Survey.

US Environmental Protection Agency and the US Geological Survey (2012). *National hydrography dataset plus – NHDPlus (Version 2.1)*. Washington, DC: U.S. Government. Retrieved from http://www.horizon-systems.com/NHDPlus/index.php

Wagenbrenner, J. W., MacDonald, L. H., & Rough, D. (2006). Effectiveness of three post-fire rehabilitation treatments in the Colorado Front Range. *Hydrological Processes*, *20*, 2989–3006. https://doi.org/10.1002/hyp.6146

Wagenbrenner, J. W., & Robichaud, P. R. (2014). Post-fire bedload sediment delivery across spatial scales in the interior western United States. *Earth Surface Processes and Landforms*, *39*, 865–876. https://doi.org/10.1002/esp.3488

Warziniack, T., & Thompson, M. (2013). Wildfire risk and optimal investments in watershed protection. *Western Economics Forum*, *12*(2), 19–28.

Wilson, C., Kampf, S. K., Wagenbrenner, J. W., & MacDonald, L. H. (2018). Rainfall thresholds for post-fire runoff and sediment delivery from plot to watershed scales. *Forest Ecology and Management*, *430*, 346–356. https://doi.org/10.1016/j.foreco.2018.08.025

Winchell, M. F., Jackson, S. H., Wadley, A. M., & Srinivasan, R. (2008). Extension and validation of a geographic information system-based method for calculating the Revised Universal Soil Loss Equation length-slope factor for erosion risk assessments in large watersheds. *Journal of Soil and Water Conservation*, *63*, 105–111. https://doi.org/10.2489/JSWC.63.3.105

Writer, J. H., Hohner, A., Oropeza, J., Schmidt, A., Cawley, K. M., & Rosario-Ortiz, F. L. (2014). Water treatment implications after the High Park Wildfire, Colorado. *Journal of the American Water Works Association*, *106*(4), 189–199. https://doi.org/10.5942/jawwa.2014.106.0055

Table A.1. For Forests (≥ 10% LANDFIRE canopy cover), the *C* factor was Changed to the Mean Postfire Values by Burn Severity from Larsen and MacDonald (2007). Proportional Adjustment Factors were Used to Estimate the Postfire *C* Factor for Nonforest (< 10% LANDFIRE Canopy Cover) and the Postfire *K* Factor for all Vegetation Types

Severity	Forest *C*	Nonforest *C* Adjustment Factor	*K* Adjustment Factor
Low	0.01	1.20	1.50
Moderate	0.05	1.50	1.75
High	0.20	2.00	2.00

APPENDIX A

A1. Hillslope Erosion

Postfire increase in hillslope erosion was modeled with a GIS implementation (Theobald et al., 2010) of the Revised Universal Soil Loss Equation (RUSLE; Renard et al., 1997). RUSLE predicts gross erosion (Mg/ha/yr) as the product of factors for rainfall erosivity (*R*), soil erodibility (*K*), length and slope (*LS*), cover (*C*), and support practices (*P*). Undisturbed erosion rates are generally not problematic in the study water system, so our assessment focused on the fire-related increase in erosion. *R* comes from the stochastic series of rainfall erosivity described previously. *LS* for both conditions was calculated using terrain analysis of a 30-m resolution digital elevation model (USEPA and USGS, 2012) per Winchell, Jackson, Wadley, and Srinivasan (2008) with modifications to limit the maximum hillslope length to 300 m and the resulting *LS* factor to 72.15 based on the range of values suggested in Renard et al. (1997). Prefire *K* was mapped using attributes for the top 15-cm of soils from the soil survey geographic database (SSURGO) where available and the state soil geographic database (STATSGO) to fill missing data (NRCS Soil Survey Staff, 2016). Prefire *C* was assigned by existing vegetation type from LANDFIRE (2016) using previously reported values from the literature as described in Gannon et al. (2019). *K* and *C* factors were varied based on wildfire extent and burn severity (Table A.1; Gannon et al., 2019; Larsen & MacDonald, 2007) to represent the primary effects of fire on soils and surface cover (Larsen et al., 2009; Shakesby & Doerr, 2006). No support practices were considered to model the unmitigated erosion hazard.

For each fire, the increase in erosion was tracked over the first three postfire years. We estimate that with constant rainfall, erosion in year two should be 15% lower than in year one and erosion in year three should be 75% less than year one, based on the rate of surface cover recovery and its influence on erosion (Benavides-Solorio & MacDonald, 2005; Larsen et al., 2009; Pietraszek, 2006). Therefore, annual fire-related erosion (A_y) was calculated with a recovery adjustment factor, RAF, of 1, 0.85, and 0.25 for postfire years one through three respectively (Equation A.1)

$$A_y = R_y \times \mathrm{LS} \times [(K_b \times C_b) - (K \times C)] \times \mathrm{RAF}_{pfy} \quad \text{(A.1)}$$

The subscript *y* is the index for the common fire and rainfall simulation year, the subscript *b* indicates the burned condition for *K* and *C* factors, and *pfy* is the index for time since fire starting at one for the fire year. RUSLE can predict unrealistic erosion rates on very steep, long slopes, so we limited annual erosion to 100 Mg/ha/yr based on previous hillslope erosion observations from the study region (Moody & Martin, 2009).

A2. Hillslope Sediment Transport

The proportion of eroded hillslope sediment delivered to streams was estimated with an empirical model of postwildfire hillslope sediment delivery ratio (*hSDR*) from the western United States (Wagenbrenner & Robichaud, 2014). First, the NHDPlus stream channel network was extended to include all pixels with a contributing area greater than 10.8 ha (Henkle, Wohl, & Beckman, 2011) because the flowline network does not consistently include many of the lowest order channels. The annual length ratio model from Wagenbrenner and Robichaud (2014) (Equation A.2) was then applied to estimate postfire *hSDR* based on the flow path length from each pixel to the nearest stream channel as the "catchment length" and the flow path length across the pixel as the "plot length" from terrain analysis of the NHDPlus 30-m resolution DEM in ArcGIS 10.3 (ESRI, 2015). To better align our net sediment yields with observations from small catchments in Colorado (Wagenbrenner & Robichaud, 2014), we doubled the resulting *hSDR*, which increased the maximum

Table A.2. Summary Statistics of First-Year Postfire Erosion and Sediment Delivery to Streams (Mg/ha/yr) for the Portion of Wildfires that Burned the Study Watershed in Three Categories Rainfall Erosivity. These are Total Sediment Yields Including the Coarse and Fine Fractions

	<500 MJ mm ha^{-1} h^{-1}		500-1,000 MJ mm ha^{-1} h^{-1}		> 1,000 MJ mm ha^{-1} h^{-1}	
	n = 3,738 Fires		n = 1,496 Fires		n = 507 Fires	
Statistic	Erosion	To Streams	Erosion	To Streams	Erosion	To Streams
Lower decile	1.9	0.9	5.2	2.5	12.7	6.1
Lower quartile	5.7	2.8	14.6	7.2	27.5	14.3
Median	13.6	6.7	30.4	15.1	50.7	25.0
Mean	18.1	9.0	32.6	16.3	49.5	24.5
Upper quartile	26.3	13.1	48.0	24.0	70.1	34.3
Upper decile	40.5	19.8	64.2	31.3	85.8	41.3

hSDR from 0.27 to 0.54 for areas near streams and increased the minimum hSDR from 0.05 to 0.10 for locations furthest from streams. Channel pixels were assigned *hSDR* of 1

$$\log(hSDR) = -0.56 - 0.0094 \times \left(\frac{\text{Flow path length to nearest channel}}{\text{Flow path length across pixel}}\right). \quad \text{(A.2)}$$

The annual mass of fire-related sediment (Mg delivered from a catchment to the stream network (TS_y) was calculated as the sum product of the annual hillslope erosion rate (A_y), the pixel area, and *hSDR* for all burned pixels (N) in the catchment (Equation A.3).

$$\text{TS}_y = \sum_{i=1}^{N} A_{y,i} \times 0.09\frac{\text{ha}}{\text{pixel}} \times hSDR_i \quad \text{(A.3)}$$

A3. Channel Sediment Transport

A channel sediment delivery ratio (*cSDR*) model adapted from Frickel et al. (1975) was used to predict the proportional throughput of sediment for flowlines (channels) based on stream order (Gannon et al., 2019). Transport of sand and smaller sediments should be efficient based on postfire observations of sediment transport in the study region (Miller et al., 2017; Moody & Martin, 2001; Ryan et al., 2011). Low order channels in the study area are characterized by ephemeral or intermittent flow and high roughness from coarse bed material and streamside vegetation. The highest order channels are still steep mountain streams with considerably greater transport capacity due to higher magnitude perennial flows. To approximate these trends, *cSDRs* of 0.75, 0.80, 0.85 and 0.95 per 10 km of stream length were assigned to first, second, third, and fourth or higher-order streams, respectively. The terminal flowlines in lakes and reservoirs were assigned *cSDR* of 0.05 to reflect that most sediment will be trapped. The annual mass of fire-related sediment (Mg) delivered to a water supply (TWS_y) was calculated as the sum of sediment delivered to streams for all upstream catchments multiplied by the product of *cSDRs* for the intervening flowlines (Equation A.4).

$$TWS_y = \sum_{j=1}^{O}(TS_{y,j} \times \prod_{k=1}^{P} cSDR_k), \quad \text{(A.4)}$$

The subscript j is the index for the O upstream catchments and the subscript k is the index for the

P intervening flowlines between catchment *j* and the water supply.

A4. Model Evaluation

Our fire-level predictions of first-year postfire erosion and net sediment delivery to streams are close to the ranges reported for previous fires in the Colorado Front Range. At lower rainfall erosivity, our simulated erosion rates (Table A.2) are near the study-wide means of 9.5–22.2 Mg/ha/yr and the range of individual hillslope observations of 0.1–38.2 Mg/ha/yr reported for most fires in the region (Larsen et al., 2009; Robichaud, Lewis et al., 2013; Schmeer et al., 2018; Wagenbrenner et al., 2006). Approximately 25% of fires exposed to higher rainfall erosivity (Table A.1) meet or exceed the 72 Mg/ha/yr of rill and interrill erosion observed in response to extreme rainfall following the Buffalo Creek Fire (Martin & Moody, 2001; volume estimates converted with bulk density of 1.6 Mg/m). Few fires are predicted to deliver sediment to streams at the maximum rates of 22.0–38.6 Mg/ha/yr observed from small catchments in the first two years after the Hayman Fire (Robichaud, Wagenbrenner et al., 2013; Robichaud, Wagenbrenner, Brown, Wohlgemuth, & Beyers, 2008) unless exposed to high rainfall erosivity (Table A.1). The channel transport losses further lower sediment yields, so none of the simulated fires at any rainfall level are expected to reach the normalized reservoir input of 52.5 Mg/ha/yr from the Buffalo Creek Fire (Moody & Martin, 2001).